

Myoglobin Diffusion in Bovine Heart Muscle

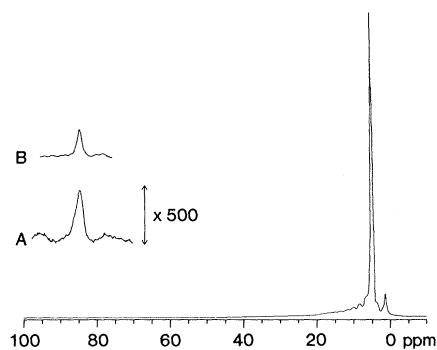
Abstract. *The rotational mobility of myoglobin in situ was determined by proton nuclear magnetic resonance line width measurements of a characteristic myoglobin resonance observed in bovine heart muscle spectra. The protein diffuses intracellularly at nearly half the rate observed in dilute solution. This high mobility allows the oxygenated form of myoglobin to contribute significantly to the overall diffusive flux of oxygen in respiring heart muscle.*

Myoglobin (Mb) is an oxygen-binding heme protein found in the heart and skeletal muscle of vertebrates. Its function in muscle is poorly understood. Recent evidence for a facilitation of intracellular oxygen diffusion by Mb has been based on in situ inactivation of the protein and measurement of the resulting decrease in steady-state respiration of the tissue (1, 2). Nevertheless, a direct calculation of the contribution of facilitated diffusion to the overall oxygen flux requires knowledge of the in situ diffusion constant of Mb (2). Nuclear magnetic resonance (NMR) is a noninvasive technique capable of yielding dynamic information on the molecule. The unique paramagnetism of the deoxy form of Mb causes an easily identified resonance of the proximal histidyl exchangeable N₈ proton to occur outside of the normal diamagnetic region of the ¹H-NMR spectrum. The field dependence of the line width of this peak makes it possible to determine the rotational correlation time (τ_r) of the protein in situ, which is at maximum 2.3 times greater than that of the protein in dilute solution.

A bovine heart received immediately after slaughter was transported to the laboratory in 0.25M sucrose on ice. A section of the heart wall muscle free of connective tissue was taken at 2°C and inserted into a 12-mm NMR tube which was fitted with a small capillary to allow displaced air to escape. The section was covered with 2 ml of a Ringer-Locke solution, and the tube was flushed with nitrogen to remove oxygen from the headspace. The purplish color of the sample was indicative of deoxymyoglobin (deoxyMb), which was expected as the dominant Mb form in respiring muscle under the anaerobic conditions in the tube. All muscle spectra were taken within several hours of receipt of the heart. Cardiac muscle is rich in oxidative (type I) muscle fibers which do not undergo significant alterations in structural integrity over several days time, as shown for these fibers in bovine longissimus muscle (3). Excised bovine muscle has been shown to maintain high activities of several marker enzymes, such as nucleosidetriphosphotases (4), for extended periods. Bovine Mb was purified

according to the procedures described by Hagler *et al.* (5). The resulting met-myoglobin, in a 10 percent D₂O solution, was reduced and deoxygenated under N₂ by sodium dithionite immediately prior to the experiment. The ¹H-NMR spectra were obtained at 200 and 360 MHz. Solution spectra were obtained at low Mb concentration (0.5 mM) to minimize viscosity effects.

Myoglobin in the red-muscle fiber is unique in that ¹H-NMR can be used to measure its mobility in situ, whereas similar studies would be unlikely for other proteins. Structural and membrane-bound proteins display large inhomogeneity and dipolar broadening. Although most soluble proteins are found at concentrations well below those (~ 1 mM) required to overcome the insensitivity of the NMR technique, Mb concentrations in mammalian red muscle tissue range from 0.1 to 0.5 mM. The paramagnetism of deoxyMb gives rise to a uniquely resolvable proton resonance due to the large hyperfine shift experienced, and the rapid electron spin relax-

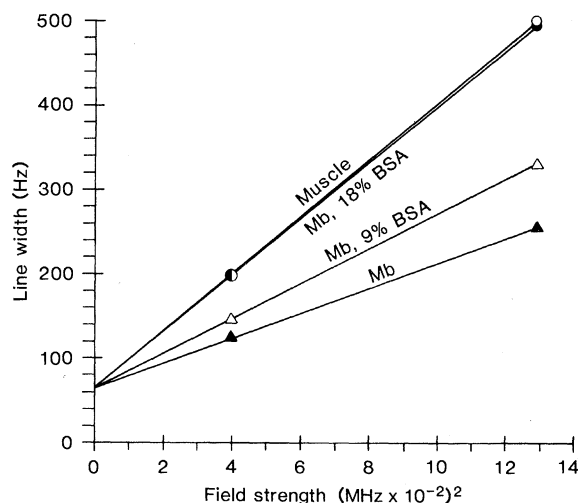


ation characteristics of the high-spin ferrous porphyrin lead to a quadratic field-dependent relaxation mechanism (Curie spin relaxation) which directly yields the correlation time of rotational diffusion of the whole protein. The ¹H-NMR spectra of numerous high-spin ferrous proteins in nonviscous solution have demonstrated that the exchangeable proximal histidyl imidazole proton resonates in a unique window at ~ 80 parts per million (ppm) from the large diamagnetic envelope region which contains most of the resonances of all other mobile proton signals.

Figure 1 shows the ¹H-NMR spectrum of the muscle sample. The water peak at ~ 5 ppm dominates the spectrum, along with a high-field shoulder peak, probably due to aliphatic carbon protons from mobile lipid or protein components. However, a broad peak is visible at ~ 80 ppm. This peak coincides with the previously assigned (6) proximal imidazole exchangeable N₈ proton found in the spectrum of purified bovine Mb in solution, which is also shown in Fig. 1. A variation in sample temperature from 25° to 13°C produced identical ~ 3 ppm downfield shifts in both the solution and the muscle. Comparison of the peak area for the muscle spectrum with a 0.20 mM bovine Mb solution, which corresponds to the Mb concentration we measured in the muscle by conventional extraction techniques and visible spectrophotomet-

Fig. 1. The ¹H-NMR spectrum of bovine heart muscle and bovine Mb solution at 13°C. The predominant resonance at ~ 5 ppm is the H₂O peak. Insets show the proximal histidyl exchangeable N₈ proton resonance after a 500-fold expansion of the muscle spectrum (A) and the corresponding resonance in a 0.75 mM bovine Mb solution spectrum (B). All solutions contained 10 percent D₂O to provide a field-position lock for the spectrometer. The pH of the bovine Mb solutions was measured under N₂ with a Beckman model 3500 pH meter equipped with an Ingold microcombination electrode. No correction was made to the measured pH values for the 10 percent D₂O in the sample. Muscle spectra were acquired without field-lock signal. All spectra were acquired on Nicolet 200- and 360-MHz spectrometers in the Fourier transform mode with the use of quadrature detection. Solution spectra required ~ 10,000 transients for good signal-to-noise ratios, whereas muscle spectra required 50,000 to 100,000 transients. For integration of the exchangeable proton resonance, we collected spectra at 200 MHz into 4096 data points, using a presaturation pulse of 60 msec applied to the H₂O signal followed by a 25- μ sec 90° tipping pulse and a 51-msec acquisition time. The signal-to-noise ratio was enhanced by introduction of a 50- to 100-Hz line broadening, via exponential multiplication of the free induction decay (FID) prior to Fourier transformation. Account was made in calculation of in situ Mb concentration for the different number of transients required for the muscle spectra. Spectra used for the line width determination were collected at 25°C into 8192 data points with a "2-1-4" Refield observation pulse train (17) centered at ~ 100 ppm, with the sweep width set to fold in the H₂O resonance at the edge of the spectrum (± 20 kHz at 200-MHz field strength). This precise setting of the sweep width greatly decreased baseline roll and carrier pulse breakthrough. The tipping pulse was precisely adjusted under manual control via an analog-to-digital converter and potentiometer to minimize the components of the H₂O in the FID. Line widths were determined by computer line-fitting routines (NTCCAP) available in the Nicolet NTC-1180 data system used for processing the spectra. Allowance was made for the artificially introduced line broadening.

Fig. 2. Variation of the line widths for bovine Mb in solution, bovine heart muscle and bovine Mb in the presence of bovine serum albumin, BSA, all at 25°C. The resonance line widths of the proximal histidyl N_δ proton are plotted versus the square of the field strength. These field strength units are converted to Hz/(gauss)² for cgs (centimeter-gram-second) unit calculations, based on Eq. 2. At least two line width determinations were made for each point, and the mean values were used for calculations. Linear regression line fits were performed in calculating the slopes. Errors for each data point are ~ 15 percent, with the variation dominated by uncertainties in the phasing and line-fitting procedures as opposed to sample-to-sample variations. Error bars are omitted for clarity.



ric quantitation, indicates that within experimental error (~ 10 percent) all of the Mb in the muscle is being observed. Spectra used for integration were acquired with the use of a 90° tipping angle and long repetition time to minimize T_1 (spin lattice relaxation time) discrimination. In addition, the solution conductivity was adjusted to produce identical radio-frequency losses as in the muscle, thus providing similar probe tuning and sensitivity.

The chemical shift and line width of the peak exclude the corresponding histidyl peaks in deoxyhemoglobin (deoxyHb) as its origin, since bovine hemoglobin was determined to have comparable peaks at 61 and 75 ppm (for the α and β chains, respectively) with line widths 300 Hz greater than that of the observed muscle peak (4). Because deoxyHb is below the limit of detection in situ, these resonances are not detected in the muscle spectrum.

Figure 2 shows the field dependence of the line width in bovine Mb in solution and in situ. Dipolar relaxation in paramagnetic compounds has two contributions. The affected nucleus relaxes in response to the field created by the fluctuating part of the instantaneous electronic spin and by the averaged or "Curie" spin. The latter is modulated only by the rotational motion of the molecule. These two effects on the observed line width, L_w , are expressed as (7):

$$L_w = \left(\frac{7}{15} \gamma^2 \mu_{\text{eff}}^2 r^{-6} \right) T_{1c} + \left(\frac{4\gamma^2 \mu_{\text{eff}}^4 r^{-6} B_0^2}{45k^2 T^2} \right) \tau_r \quad (1)$$

where γ is the magnetogyric ratio, μ_{eff} is the effective magnetic moment, r is the Fe- N_δ -H distance, T_{1c} is the electronic

relaxation time, B_0 is the applied magnetic field, k is Boltzmann's constant, T is the absolute temperature, and τ_r is the rotational correlation time for the protein. Equation 1 was obtained from the original equation of Gueron (7) with the terms expanded as described (8). For rapid-spin electron relaxation (very short T_{1c}), as found in deoxyMb, and for slow rotational diffusion, as found for proteins even in dilute solution, the first term in Eq. 1 is field-independent but the second term (Curie spin) shows quadratic field dependence. The slope of a plot of line width versus magnetic field strength, (B_0^2), is given by

$$\text{slope} = \frac{4\gamma^2 \mu_{\text{eff}}^2 \tau_r}{45\pi k^2 T^2 r^6} \quad (2)$$

Such quadratic field dependence has been observed for deoxyMb, deoxyHb (9), and cytochrome c' (10), and in this work for the exchangeable proton resonance of sperm whale deoxyMb by line width measurements at 100, 200, and 360 MHz. The line widths of bovine Mb and bovine heart muscle spectra were determined at 200 and 360 MHz. The extrapolated zero-field line widths for each sample were identical within experimental error, verifying the quadratic field dependence for the protein. Knowledge of μ_{eff} and r (from x-ray crystallographic data coordinates) allows calculation of τ_r . The value of r was estimated to be 5.1 Å from a three-dimensional molecular model of sperm whale Mb, obtained from the laboratory of Kendrew (11). Then τ_r is calculated for sperm whale Mb as 5.3 nsec and for bovine Mb as 6.4 nsec, values consistent with the 6.5 nsec measured for sperm whale Mb at 29°C from the ¹H-NMR field dependence of the heme methyl peaks (9) and a τ_r of 10.3 nsec at 15°C measured by polariza-

tion of fluorescence (12). The similar values of τ_r we observe for sperm whale Mb and bovine Mb are expected from the similar masses (17,199 and 16,901 daltons, respectively) and hydrodynamic properties (13) of these proteins.

The apparent τ_r of bovine Mb in situ is 15 nsec, roughly 2.5 times longer than in dilute solution. This value represents an upper limit for τ_r since inhomogeneity or dipolar broadening of the peak would contribute to the observed line width. The addition of 9 or 18 percent bovine serum albumin (BSA) to our dilute Mb solutions increases the observed line widths and calculated τ_r values to 9.0 and 14 nsec, respectively. The viscosities of these solutions were measured with an Ostwald viscometer, and the resulting relative viscosity (η_{rel}) was compared to the τ_r of bovine Mb solution. Ratios of η_{rel} (BSA/dilute Mb solution) were, respectively, 1.5 and 2.7 for the 9 and 18 percent BSA solutions, and the corresponding τ_r ratios were 1.4 and 2.3, respectively. The τ_r thus reflects the overall solution viscosity, which we estimate for the sarcoplasm as approximately 2.5 centipoise.

The function of Mb in the muscle fiber has been poorly understood; Mb has traditionally been labeled an oxygen storage protein that increases the oxygen capacity of the tissue. Studies of respiration rate carried out under steady-state oxygen supply conditions on several red muscle systems, including pigeon muscle fiber bundles (14) and chicken gizzard smooth muscle (1), have suggested a dynamic role for Mb in muscle respiration. Below limiting oxygen pressures (150 mmHg), Mb has been shown to facilitate oxygen diffusion to approximately twice the level observed when the protein is inactivated (14). The conditions for facilitated diffusion of Mb have been described as follows (15): (i) sufficiently low intracellular oxygen tension (pO_2) to allow deoxyMb to exist in vivo; (ii) a gradient of MbO₂ to be formed to provide a driving force for facilitated diffusion; and (iii) sufficient mobility of the MbO₂ to permit diffusion of the oxygen carrier. Although the first two conditions have been verified experimentally, the third condition has been implied by physiological studies but not directly measured as far as we know.

The ability to detect unambiguously an NMR signal for Mb in situ may have direct clinical applications. Measurement of MbO₂/deoxyMb ratios by integration of the observed peak affords direct estimation of the pO_2 of skeletal and heart muscle. A recent report of such a measurement by visible reflectance

spectrophotometry of perfused rat heart provides valuable information on changes in pO_2 during contraction (16). The NMR method is potentially superior, however, because it is applicable to intact organs in vivo by use of topological surface probes. The method may be especially useful in monitoring the effects of perfusates designed to maintain aerobic conditions in the heart. In addition, the effects of oxidant drugs in inducing metmyoglobinemia may be followed, as the spectrum of metmyoglobin also shows characteristic resonances in the paramagnetic region.

DAVID J. LIVINGSTON

*Institute of Marine Resources,
University of California, Davis 95616*

GERD N. LA MAR

*Department of Chemistry,
University of California, Davis*

W. DUANE BROWN

*Institute of Marine Resources,
University of California, Davis*

References and Notes

1. J. de Koning, L. J. C. Hoofd, F. Kreuzer, *Pfluegers Arch.* **389**, 211 (1981).
2. R. P. Cole, *Science* **216**, 523 (1982).
3. G. L. Gann and R. A. Merkel, *Meat Sci.* **2**, (No. 2), 129 (1978).
4. R. M. Robson, D. E. Goll, M. J. Main, *J. Food Sci.* **32**, 544 (1967).
5. L. Hagler, R. I. Coppes, Jr., R. H. Herman, *J. Biol. Chem.* **254**, 6505 (1979).
6. G. N. La Mar, D. L. Budd, H. Goff, *Biochem. Biophys. Res. Commun.* **77**, 104 (1977).
7. M. Gueron, *J. Magn. Reson.* **19**, 58 (1975).
8. The terms from Gueron (7), equation 15, have been expanded as follows:

$$\Delta = \frac{\gamma g \beta}{r^3} \text{ (cgs units)}$$

where g is the spectroscopic splitting factor and β is the Bohr magneton.

$$S_c = g\beta S(S+1) \frac{B_0}{3kT} = \frac{\mu_{\text{eff}}^2 B_0}{3g\beta kT}$$

[since $\mu_{\text{eff}} = g\beta[S(S+1)^{1/2}]$ where S is the spin quantum number.

$$\frac{1}{T_2} = \left(\frac{\Delta^2 S_c^2}{5}\right) 4\tau_r + \frac{7}{15} \Delta^2 S(S+1) T_{1c} (\omega_1^2 \tau_r^2 \gg 1)$$

where T_2 is the spin-spin relaxation time and ω_1 is the proton Larmor frequency.

9. M. E. Johnson, L. W. M. Fung, C. Ho, *J. Am. Chem. Soc.* **99**, 1245 (1977).
10. G. N. La Mar, J. T. Jackson, R. G. Bartsch, *ibid.* **103**, 4405 (1981).
11. J. C. Kendrew, R. E. Dickerson, B. E. Strandberg, R. G. Hart, D. R. Davis, D. C. Phillips, V. C. Shore, *Nature (London)* **185**, 422 (1960).
12. S. R. Anderson, M. Brunori, G. Weber, *Biochemistry* **9**, 4723 (1970).
13. M. Z. Atassi, *Biochim. Biophys. Acta* **221**, 612 (1970).
14. B. A. Wittenberg, J. B. Wittenberg, P. R. B. Caldwell, *J. Biol. Chem.* **250**, 9038 (1975).
15. J. B. Wittenberg, *Physiol. Rev.* **50**, 559 (1970).
16. I. E. Hassinen, J. K. Hiltunen, T. E. S. Takala, *Cardiovasc. Res.* **15**, 86 (1981).
17. A. G. Redfield, S. D. Kunz, E. K. Ralph, *J. Magn. Reson.* **19**, 114 (1975).
18. We acknowledge useful discussions with and technical assistance provided by J. T. Jackson and G. B. Matson. All spectra were acquired on instrumentation of the University of California at Davis NMR facility. This research was supported by grants from the National Institute of Health (G.N.L.), the Sea Grant Program (W.D.B.), and the University of California at Davis NMR facility.

14 May 1982; revised 8 September 1982

Blood Cell Surface Changes in *Drosophila* Mutants with Melanotic Tumors

Abstract. *When wheat germ agglutinin conjugated to fluorescein isothiocyanate is bound to hemocytes from larvae of Drosophila melanogaster, two populations of hemocytes are distinguished. One shows a fluorescent speckled surface (spk⁺) and the other lacks this characteristic (spk⁻). In mutant larvae with melanotic tumors and in larval hosts with heterospecific implants, most of the lamellocytes (a hemocyte variant involved in capsule formation and tissue rejection) are spk⁺, whereas the lamellocytes in nontumorous larvae are spk⁻. This suggests that spk⁺ lamellocytes are necessary for encapsulation of aberrant tissues in the mutant larvae and are responsible for rejection of foreign tissue implants.*

Subpopulations of vertebrate lymphocytes have been recognized and separated by use of plant lectins specific for carbohydrate moieties on the cell surfaces (1). Immunocompetent cells are distinguishable from immature cells by these methods. Although insects lack an immune system capable of antibody production, their blood cells do recognize foreign substances (2). Insect hemocytes readily phagocytize bacteria and small particulate materials that enter the hemocoel. Larger foreign objects are surrounded by layers of flattened hemocytes, known as lamellocytes, that adhere to each other, forming compact melanized capsules. In *Drosophila melanogaster*, encapsulation is also used to enclose aberrant tissues in mutant strains that develop melanotic tumors (3) and for rejection of heterospecific tissue implants (4).

Capsule formation requires binding between lamellocytes that previously existed as separate cells in the hemocoel. Therefore, the surfaces of the lamellocytes adhering to each other during encapsulation of a foreign object must be altered so that they have adhesive sites or adhesive materials. If this is so, then lamellocytes stimulated to form capsules in the mutants with melanotic tumors should be distinguishable from lamellocytes not actively engaged in such a response. To test this possibility we used a temperature-sensitive mutant strain that develops melanotic tumors at permissive temperature. Wheat germ agglutinin (WGA) conjugated to fluorescein isothiocyanate was used to show binding to lamellocytes. The percentage of lamellocytes showing WGA binding as a speckled surface (spk⁺) was increased at the tumor-permissive temperature; these

Table 1. Blood cell response to wheat germ agglutinin. Data from nontumorous and tumorous larvae were obtained from two samples of hemocytes each taken from a pool of hemolymph from three specimens (except *Ore-R* lamellocyte counts, which were taken from four to six samples). Since data from the samples in each group were consistent ($P > .5$; χ^2_{df}), they were pooled. Samples from four nontumorous larvae with *Drosophila virilis* implants were grouped into two consistent pools. Larvae were grown at temperatures used previously to study melanotic tumor formation or to study the blood cells of each strain (3, 5). N.D., none detected.

Strain, temperature, and age	Cell type	Number of cells	Percentage of spk ⁺ forms
<i>Nontumorous larvae</i>			
<i>Ore-R</i>			
26°C, 72 hours	Lamellocyte	22	N.D.
26°C, 88 hours	Lamellocyte	60	N.D.
26°C, 72 hours	Plasmatocyte	833	N.D.
<i>tu-Sz^{ts}</i>			
18°C, 6 days	Lamellocyte	470	3
18°C, 7 days	Lamellocyte	234	5
18°C, 6 days	Plasmatocyte	600	< 0.01
<i>Tumorous larvae</i>			
<i>tu-Sz^{ts}</i>			
26°C, 50 hours	Lamellocyte	247	81
26°C, 72 hours	Lamellocyte	179	79
26°C, 72 hours	Plasmatocyte	984	12
<i>tu-W</i>			
24°C, 72 hours	Lamellocyte	210	46
24°C, 90 hours	Lamellocyte	276	62
<i>tu bw</i>			
24°C, 72 hours	Lamellocyte	218	72
<i>Nontumorous larvae with D. virilis implants</i>			
<i>tu-Sz^{ts}</i>			
18°C*	Lamellocyte	196	71
18°C*	Lamellocyte	392	53

*Host age was 6 days, and hemocytes were sampled 26 hours later.